Sustainable Energy & Fuels

Interdisciplinary research for the development of sustainable energy technologies

Accepted Manuscript

This article can be cited before page numbers have been issued, to do this please use: D. Bardgett, J. Ho, D. Swearer and S. M. Haile, *Sustainable Energy Fuels*, 2026, DOI: 10.1039/D6SE00290K.

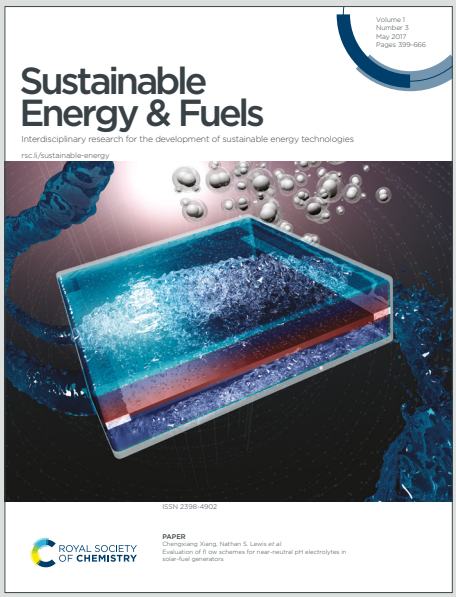

ROYAL SOCIETY OF CHEMISTRY

rsc.li/sustainable-energy

View Article Online
DOI: 10.1039/D6SE00290K

Plasma-coupled Electrochemical Ammonia Synthesis Using a Solid Acid Electrochemical Cell

Dylan Bardgett,[a] *James Ho,*[b] *Dayne F. Swearer,*[a,b*] *and Sossina M. Haile*[a,c*]

[a]Department of Chemistry, Northwestern University, Evanston, IL 60208, USA

[b]Department of Chemical and Biological Engineering, Northwestern University, Evanston, IL 60208, USA

[c]Department of Materials Science and Engineering, Northwestern University, Evanston, IL 60208, USA

*Corresponding Authors: dayne.swearer@northwestern.edu, sossina.haile@northwestern.edu

Abstract

Carbon-free synthesis of ammonia is an essential component of a sustainable future. In this work, we develop a reactor utilizing a solid acid electrochemical cell coupled with an atmospheric-pressure nitrogen/argon plasma jet for the electrochemical nitrogen reduction reaction. The cell is based on the electrolyte $Cs_7(H_4PO_4)(H_2PO_4)_8$, which displays high conductivity at temperatures above 90 °C. We show that plasma-activated nitrogen species directly react with protons at the surface of the molybdenum cathode at 140 °C. Under a reducing bias of -2 V across the electrochemical cell and a plasma power consumption of 7.3 W, the plasma-coupled electrochemical route produces ammonia at a rate of 1.2 ± 0.5 nmol/s·cm^2. In the absence of the plasma, the purely electrochemical process produces negligible amounts of ammonia, comparable to the background level of 0.05 nmol/s·cm^2, underscoring the critical role of the plasma activation.

Keywords: Plasma-coupled electrocatalysis; Solid acid electrolytes; Ammonia synthesis

Introduction

Although the reaction between H_2 and N_2 to form ammonia is thermodynamically favorable at ambient pressures and temperatures, it was not until the development of the high-temperature, high-pressure Haber-Bosch process that industrial production of ammonia became feasible. Today, the Haber-Bosch process is essential for global agriculture and stands to play an important role in the future renewable energy economy.[1, 2] However, this process is only economically viable at large scales.[3] In contrast, technologies that produce ammonia (NH_3) through electrified means are a promising pathway to enable decentralized production while significantly reducing the carbon intensity associated with the manufacture of this critical commodity chemical.[4] In this context,

View Article Online
DOI: 10.1039/D6SE00290K

electrochemical NH_3 synthesis, an electrically driven process that can function at ambient pressures, has emerged as an intriguing alternative.[5] In the most direct realization of the process, protons are driven by an applied electric field across an electrolyte and react with molecular nitrogen (N_2) and electrons at the cathode of the device, in a reaction generically termed the electrochemical nitrogen reduction reaction (NRR). The protons may be generated from H_2 oxidation reaction at the counter electrode, or ideally, from water electrolysis (releasing molecular oxygen (O_2) as byproduct). A key requirement for the success of this approach is that N_2 reduction at the cathode outcompetes the hydrogen evolution reaction (HER), the dominant, yet undesired, side reaction when protons are exposed to electrochemically reducing conditions at a cathode. While many studies have focused on screening NRR catalysts in aqueous, either acidic or basic, electrolytes, N_2 activation at the ambient temperatures required by these electrolytes has proven to be extremely difficult, and reported synthesis rates, which often barely exceed background levels of NH_3 in the atmosphere, have been brought into question.[6-10] Recent advances, however, challenge the assumption that N_2 cannot be activated under ambient conditions.[11]

One method to enhance N_2 activation over electrocatalytic surfaces is to leverage reactive nonthermal plasmas. Nonthermal plasmas are characterized by electron temperatures far greater than the average temperature of the bulk gas. In this state, high-energy electrons can collide with other species in the plasma, generating electronically and vibrationally excited molecules, ions, and free radicals.[12] In N_2 containing plasmas, molecular and electronic excitations can activate strong $N \equiv N$ bonds, enabling nonequilibrium catalytic pathways for N_2 activation.[13] While plasma-assisted NH_3 synthesis in packed-bed reactors have received significant attention,[13-15] studies aiming to utilize plasmas in conjunction with electrochemical synthesis, which offers the possibility of a second lever for controlling reaction outcomes, are more limited. A key challenge emerges in the case of aqueous electrolyte electrochemical systems, in that plasma activation of water can lead to competing oxidation reactions.[16, 17] This complexity precludes the design of a single, optimal electrocatalyst and impedes control of the reaction outcome. Additionally, use of an aqueous electrolyte necessitates energy-intensive product separation processes.[18] In contrast, the use of a solid electrolyte, in which N_2 gas is directly supplied to the cathode, overcomes these challenges. Solid proton conducting electrolytes also offer the opportunity to raise the temperature above ambient conditions, inherently enhancing catalysis rates, though in the absence of pressure, temperatures above ~ 350 °C are thermodynamically unfavorable for ammonia synthesis.

To date, there have been only two reports in which a nonthermal plasma has been combined with a solid proton conductor in pursuit of ammonia electrochemical synthesis. Kumari *et al.* implemented a nonthermal plasma with a polymer electrolyte membrane assembly with Pt at the cathode and recorded an ammonia formation rate of ~ 5×10^{-2} nmol/s·cm^2 under a large applied bias of 3.5 V, a result that was detectably higher than the rate of ~ 2×10^{-2} nmol/s·cm^2 measured in the absence of a voltage bias.[19] The unexpected production of ammonia in the absence of bias was attributed to plasma-activated reaction between water in the Nafion membrane and the supplied nitrogen. Sharma *et al.* exploited a high temperature ceramic membrane coupled with a low vacuum induction coil plasma to achieve higher rates of ammonia production. At an operating temperature of 500 °C, plasma power of 80 W, and current density of 80 mA/cm^2, an ammonia synthesis rate of 27 nmol/s·cm^2 was obtained using Pt as the cathode catalyst.[20] These early promising results hint at the viability of plasma-enhanced electrochemical routes in combination with solid electrolytes for ammonia production.

View Article Online
DOI: 10.1039/D6SE00290K

Herein, we demonstrate plasma-coupled electrochemical (PCE) synthesis of ammonia by exploiting the ideal properties of solid acid electrolytes, a class of proton-conducting salts which display high conductivity, often exceeding 10 mS/cm, at temperatures above a transition to a disordered state.[21] Examples include $CsHSO_4$ and CsH_2PO_4. Depending on the material and environmental conditions, the high conductivity phase is stable from as low as 90 °C to as high as 300 °C. These temperatures are ideal for NH_3 synthesis – low enough for thermodynamic favorability of the desired product[20] and high enough to provide rapid kinetics.[22] We recently reported a solid acid electrolyte with the stoichiometry $Cs_7(H_4PO_4)(H_2PO_4)_8$ (CPP) that can achieve a proton conductivity of 5.8×10^{-4} S/cm at 140 °C in a nominally dry environment and is also stable in the presence of H_2.[23] With this new electrolyte it is possible to supply dry H_2 to the anode of an electrochemical cell and directly interface a N_2-containing plasma with the cathode to produce NH_3. As the cathode electrocatalyst, we use molybdenum (Mo) due to its stability against reaction with the solid acid electrolyte at the operational conditions of interest, its facile nitridation reaction with nitrogen plasma,[24-27] and its poor activity for the HER. We demonstrate the integrated system and find that in the presence of the plasma, the NH_3 synthesis rate rivals prior literature results, whereas in the absence of plasma activation, ammonia production is below the detection limit of our analytical methods.

Plasma-Coupled Electrochemical Reactor Design and Operation

A schematic of the experimental apparatus used for plasma-coupled electrochemical ammonia production is provided in **Figure 1**. At the heart of the reactor is an electrochemical cell consisting of a CPP electrolyte supported on a multilayer anode, in which Pt/C (0.3 mg_{Pt}/cm^2) serves as the H_2 oxidation catalyst. A thin film of RF-sputtered molybdenum metal serves as the nitrogen reduction catalyst. Complete details regarding the preparation of the electrochemical cell are provided in the Supplemental Information.

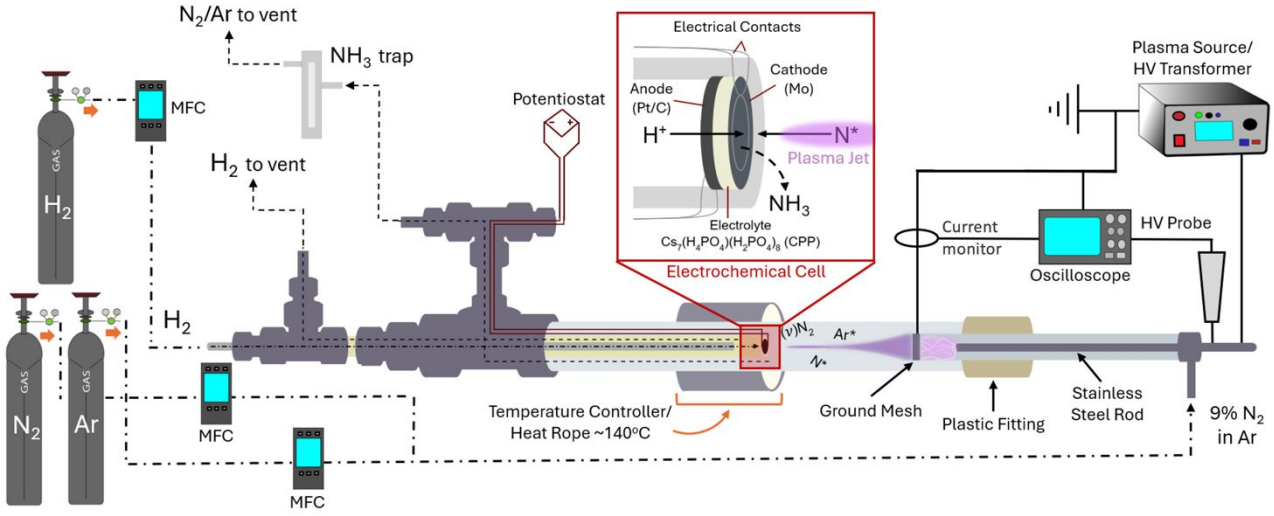

***Figure 1**. A schematic illustrating the plasma-coupled electrochemical reactor.*

Under reactor operation, protons are generated at the anode via H_2 oxidation (Eq. 1) and migrate across the electrolyte to the cathode, where they either react with N_2 to produce NH_3 (Eq.

View Article Online
DOI: 10.1039/D6SE00290K

2) or with each other to evolve H_2 gas (Eq. 3). In principle, the reaction of protons with N_2 is thermodynamically favorable (and should require no overpotential), but nitrogen dissociation is limited by a large kinetic barrier. In the PCE condition, the nitrogen in Eq. 2 can be vibrationally and electronically excited from the plasma to facilitate dissociation.

Anode: $$H_2(g) \rightarrow 2H^+ + 2e^- \quad (1)$$

Cathode: $$6H^+ + N_2(g) + 6e^- \rightarrow 2NH_3(g) \quad (2)$$

$$2H^+ + 2e^- \rightarrow H_2(g) \quad (3)$$

For integration with plasma-excited nitrogen, the solid acid electrochemical cell is mounted and sealed anode-side-down to the end of an alumina tube, with the cathode side exposed to the plasma. Both the cell and the plasma are contained within a quartz tube. The region around the cell is heated to the operating temperature using heat rope. H_2 gas is supplied to the anode side of the cell at a flow rate of 100 sccm (standard cubic centimeters per minute). At the cathode side, the gas supplied to the plasma generator is 9% N_2, balance Ar at a flow rate of 275 sccm. Argon is used as a diluent because it is much easier to ionize than N_2, allowing for stable formation of the plasma jet. Kinetic modeling has also shown that energy transfer from metastable Ar results in a significant population of vibrationally excited N_2, which has been suggested to promote N≡N bond dissociation.[28, 29] The plasma is generated using a Leap100 pulsed plasma power supply unit (PlasmaLeap). The current-voltage characteristics of the electrochemical cell are measured using a Biologic SP200 potentiostat, connected via four insulated wires that serve as the sense and power cables for the anode and cathode. Ammonia synthesis rates are quantified with the salicylate method, as described by Le and Boyd.[30] The cathode exhaust is trapped over a given period of time of reactor operation in a glass fritted bubbler filled with deionized water. A freshly prepared alkaline sodium hypochlorite solution and a sodium salicylate solution are added to a portion of the aqueous solution containing the trapped exhaust. After allowing the stirred solution to age for 1 h in a dark box, the UV-Vis absorption intensity at 651 nm is recorded and, based on a calibration, converted to the NH_3 concentration. The background NH_3 level was determined by flowing N_2/Ar gas through the reactor in the off condition; the equivalent rate was found to be 0.05 nmol $NH_3/s \cdot cm^2$. Complete details of the system design and ammonia quantification, including calibration procedures, are provided in the Supplemental Information.

Prefatory Supporting Studies

For the proposed strategy to be successful, several requirements must be met. First, activated nitrogen must have a sufficient lifetime to reach the electrochemical cell. Second, the activated nitrogen must interact with the Mo catalyst. And third, Mo must have high hydrogen diffusivity, but low HER activity, enabling hydrogen to reach the nitrogen on the catalyst surface without emerging as H_2 gas. Each of these requirements are evaluated in turn as follows.

The time-of-flight of the active species from the point of generation to impingement on the cathode was estimated from the reactor dimensions and operating parameters. From the axial flow rate of gas supplied to the plasma (275 sccm in the annular region of the plasma) and cross-sectional area (0.8 mm^2), the gas velocity is approximately 5.8 m/s. The distance from the end of the plasma jet plume to the catalyst surface is 0.64 cm, indicating a time-of-flight of ~1.1 ms. This

View Article Online
DOI: 10.1039/D6SE00290K

is shorter than the relaxation time of metastable and vibrationally excited $N_2(a')$ of ~ 0.5 s as well as that of ground state atomic $N(^4S)$ of ~ 8 ms measured in the post-discharge region of atmospheric pressure nitrogen plasmas.[31, 32] While our N_2/Ar plasma differs from the pure N_2 plasmas examined in the literature, Penning excitations of N_2 by Ar in N_2/Ar plasmas are known to increase the populations of excited nitrogen species, leading to an even higher concentration of excited nitrogen species in our PCE system.[33] If taken to decay exponentially, this analysis suggests that a significant quantity of these excited species (~99.8% of $N_2(a')$ and ~87.2% of $N(^4S)$) can survive long enough to interact with the electrode surface and promote N fixation.

Sputtered Mo films were characterized by X-ray diffraction, X-ray reflectivity, and cross-sectional scanning electron microscopy, **Figure S2**, from which phase formation was confirmed and film thickness and relative density (91%) were established. To assess the interaction of Mo with plasma-generated reactive nitrogen species, a film of Mo deposited onto Si was exposed to a N_2/Ar plasma in a simple geometry that did not prevent air from accessing the film in addition to the plasma (**Figure S3**). X-ray photoelectron spectroscopy (XPS) was used to study the Mo film before and after exposure to a 17% N_2/Ar plasma. The as-deposited film is free of any nitrogen signal (**Figure 2a**), The main Mo $3p^{3/2}$ peak at 392.2 eV is attributed to metallic Mo and a small shoulder at 395.7 eV indicates the presence of Mo^{4+} at the surface, likely due to the presence of MoO_x. Following exposure to the plasma, there is clear evidence of nitrogen in the surface region of the film as demonstrated by the appearance of the N 1s peak at 399.7 eV, **Figure 2b**. The absence of a doublet peak at 417.2 eV, 17.5 eV above the peak at 399.7 eV, supports the assignment of the 399.7 eV peak to N 1s rather than Mo 3p, which appears as $3p^{3/2}$ and $3p^{1/2}$ doublets. The surface of the Mo film is oxidized by the plasma exposure in the presence of air, with a large increase in the signal associated with Mo^{4+}. Furthermore, a small peak lying between the positions of Mo^0 and Mo^{4+} appears at 395.2 eV. In the literature, this peak is identified as $Mo^{\delta+}$, and it is often observed in the presence of nitrogen.[34] Overall, these findings indicate that molybdenum interacts with activated nitrogen species generated from N_2/Ar plasma. As Mo does not otherwise react with N_2 under ambient conditions, the incorporation of nitrogen species into the film suggests that the PCE reactor configuration will overcome slow N_2 adsorption and dissociation kinetics and provide surface nitrogen species available for electrochemical reduction. The ready oxidation of Mo in the presence of small quantities of air emphasizes the need to maintain an oxygen-free environment at the cathode. The CPP electrolyte is ideal for this application because, in contrast to the more widely implemented alternative for solid acid electrochemical devices, CsH_2PO_4,[35] CPP can be operated in its superprotonic conductivity state without need for humidification.[23]

View Article Online
DOI: 10.1039/D6SE00290K

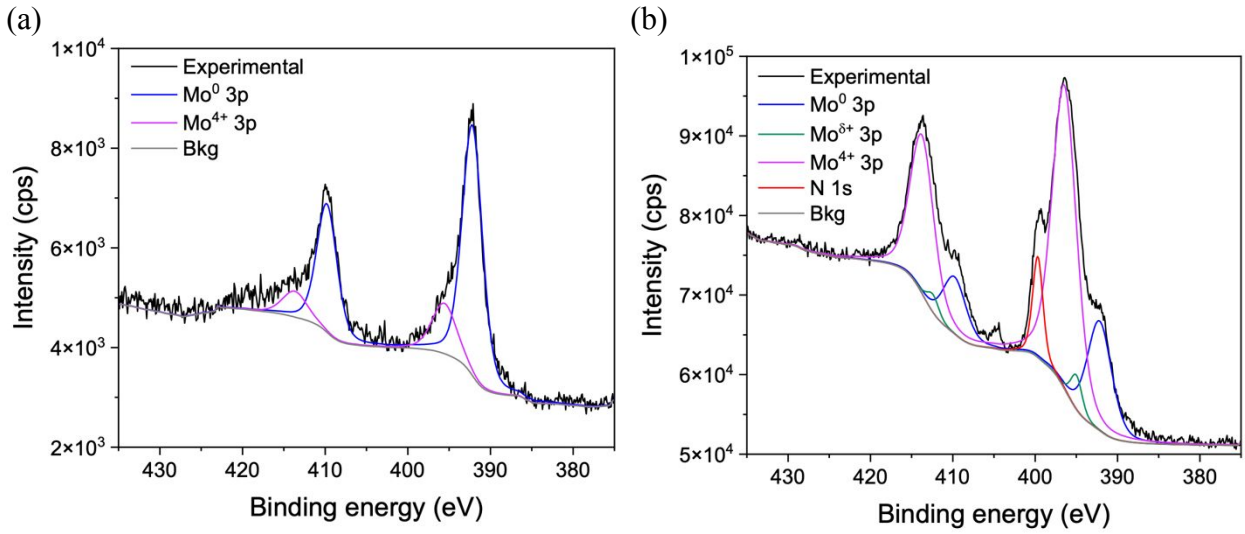

***Figure 2**. XPS characterization of Mo films (64 nm in thickness on Si) in the N 1s and Mo 3p region: (a) as-deposited; and (b) after exposure to a nitrogen plasma jet.*

The transport and catalytic properties of Mo were evaluated by measuring the electrochemical impedance of a complete cell with H_2 supplied to each electrode and comparing the response to those of cells in which the Mo electrode was either modified or replaced. If Mo is largely impermeable to hydrogen, one expects the Mo film to display a large impedance when exposed to H_2. If the impedance is due to sluggish HER kinetics at the exposed Mo-gas interface rather than sluggish kinetics at the internal Mo-electrolyte interface or slow diffusivity through the film, then one can further anticipate that contacting the Mo with a catalyst that is highly active for the HER would decrease the impedance. Accordingly, we prepared and evaluated the following two cells: one in which the Mo film was replaced with a Pt/C + CPP composite electrode (0.3 mg_{Pt}/cm^2, essentially identical to the electrode designed to serve as the H_2 oxidation catalyst in the complete cell), and one in which the Mo film was overlayed with a Pt/C + CPP composite.

The results of the impedance measurements at zero bias and 140 °C are presented in **Figure 3**, along with a representative SEM cross-section of a typical complete electrochemical cell used in the ammonia synthesis experiments. The Mo cathode exhibits an immense impedance of ~ 20 $k\Omega \cdot cm^2$ at low frequency, orders of magnitude larger than that of the standalone Pt/C cathode (1.75 $\Omega \cdot cm^2$). With the Pt/C overlayer, the electrode impedance of the cell with the Mo cathode falls to 9.1 $\Omega \cdot cm^2$, of which only 5.6 $\Omega \cdot cm^2$ is due to the introduction of Mo between the electrolyte and the Pt/C catalyst. This set of results indicates that the high impedance of the Mo film (in the absence of Pt) is due to low activity for HER at the film surface rather than poor hydrogen diffusivity through the bulk of the film. Indeed, Tanabe *et al.* have reported the hydrogen diffusivity in Mo to be ~ 10^{-5} cm^2/s at 140 °C, implying a diffusion time of just 0.1 μs through the ~ 20 nm cathode film.[36] The impedance measurements also reveal the impact of the low electronic conductivity of Mo as an additional ohmic offset, contributing ~ 20 $\Omega \cdot cm^2$ to the resistances of the cells in which Mo is the cathode.

View Article Online
DOI: 10.1039/D6SE00290K

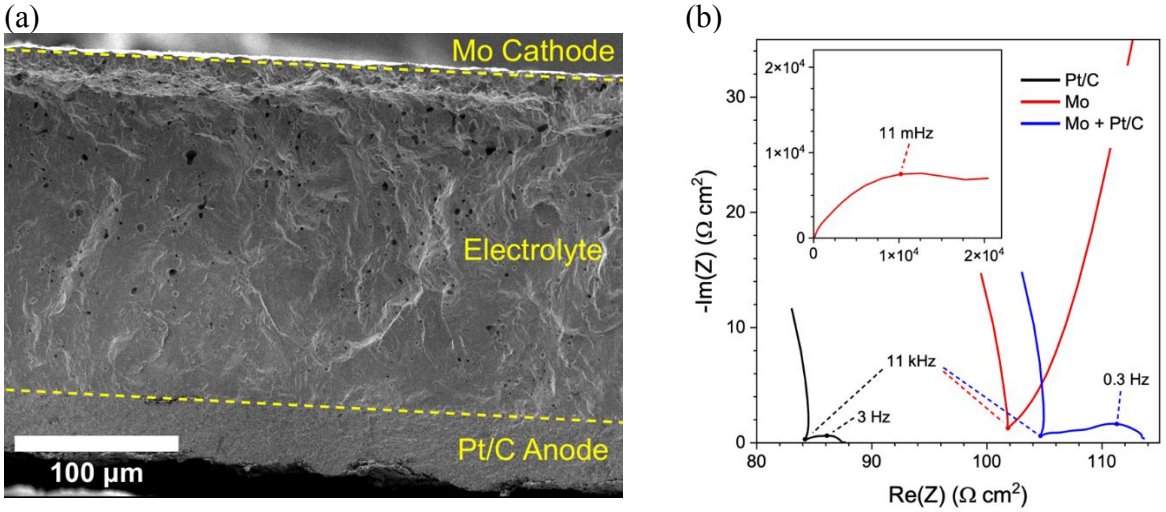

Figure 3. *Electrochemical impedance response: (a) a SEM cross-section of a representative electrochemical cell with the cell components - the 25.1 ± 0.2 nm thick Mo cathode, the 210 µm thick CPP electrolyte layer, and the Pt/C + CPP composite anode - indicated; and (b) impedance spectra collected from electrochemical cells in which one electrode was a standard Pt/C + CPP composite and the other was (i) Pt/C + CPP composite, (ii) Mo thin film (15.2 ± 0.3 nm), or (iii) a Mo thin film (15.2 ± 0.3 nm) overlayed with Pt/C + CPP composite sandwiched around a 400 µm thick CPP electrolyte layer.*

Ammonia Synthesis

The results obtained from a representative electrochemical cell with an electrolyte thickness of 210 µm, Mo cathode thickness of 25.1 ± 0.2 nm, and active area of 0.30 ± 0.01 cm^2 are reported here. The PCE reactor was operated with the electrochemical cell maintained at 140 °C, 100 sccm H_2 supplied to the anode and 275 sccm of a mixture of 9% N_2 (balance Ar) supplied to the cathode. At the initiation of the experiment, prior to plasma activation, the cell open circuit voltage was 470 mV, as compared to the infinite voltage expected, suggesting a slight leak of H_2 into the cathode chamber. The reactor was then operated with -2 V total voltage (*i.e.*, -2 V relative to the H_2 pseudo-reference at the anode). Because the impedances of the electrolyte and the anode are relatively small, **Figure 3b**, the majority of the applied voltage (~ 2.4 V including the OCV) contributes to the overpotential driving force at the cathode. In the PCE condition, the plasma was operated at 7.3 W with a pulse frequency of 500 Hz and a pulse width of 83 µsec, yielding a 4% duty cycle.

Shown in **Figure 4** are comparisons of the current density under electrochemical bias measured with and without plasma activation of N_2 at the cathode side of the reactor. In **Figure 4a**, the data are obtained with a rest period of several minutes between the plasma off and on conditions. In **Figure 4b**, the data are collected while continuously alternating between the electrochemistry only and the PCE conditions. Because the powerful, oscillating electric field from the plasma introduces substantial noise in the recorded current density, with oscillations of as much as 0.5 mA/cm^2, the data for the PCE condition (for both datasets) are smoothed. The UV-Vis absorption spectra obtained from the solutions into which the cathode exhaust was captured and processed are presented in **Figure S5**. Ammonia quantification data were collected specifically for

View Article Online
DOI: 10.1039/D6SE00290K

the experiments in which rest periods were applied between the plasma off and on conditions (**Figure 4a**).

Irrespective of the data acquisition mode (with or without rest periods), the current density is substantially higher with the plasma on than without it. For the measurements with a rest period, **Figure 4a**, in the absence of plasma activation, the current density displays a near-constant value, declining slightly from 13.6 to 12.9 mA/cm^2 over the course of the 5 min measurement. No ammonia was detected in the cathode exhaust gas above the background level, which was found to correspond to a rate of 0.05 nmol NH_3/s·cm^2. Thus, in the electrochemistry-only condition, the observed current presumably reflects hydrogen evolution from the Mo cathode. With the plasma jet on (in addition to the electrochemical bias), the initial current density (12.4 mA/cm^2) is slightly lower than without the plasma, but then continuously increases, reaching a value of approximately 22 mA/cm^2 after 5 min of operation. Significantly, NH_3 was detected in the solution used to capture the exhaust after each 5 min period of operation at a level that was substantially above the background, **Figure S5**. Here, the rate is defined simply by evaluating the total quantity of ammonia detected in the solution and normalizing it to the time of operation and the active area of the cell. NH_3 synthesis rates were measured for a total of six 5-minute intervals, alternating between pure electrochemistry and PCE conditions (with 5 – 7 minutes between off and on conditions). In all three electrochemistry-only intervals, the ammonia synthesis rate was within error of the background ammonia detection rate. With the addition of the plasma jet, the ammonia synthesis rate increased to 1.2 ± 0.5 nmol NH_3/s·cm^2, as averaged across two of the measurements, **Figure S5**. The Faradaic efficiency, defined as the fraction of current through the electrochemical cell that generates NH_3, was found to be $1.9\% \pm 0.7\%$.

The current response of the cell without rest periods between plasma off and on conditions, **Figure 4b**, reveals that the current does not immediately return to the steady state value of the electrochemistry-only condition when the plasma is turned off, mirroring the slow rise in current when the plasma is turned on. This observation suggests that the plasma generates active sites that increase in concentration towards a limiting value and which are then consumed when the plasma is off. In particular, due to the poor HER activity of Mo (**Figure 3b**), hydrogen can be expected to accumulate on the cathode surface under the electrochemistry only condition. When the plasma is turned on, processes such as electron stimulated desorption (ESD) and ion impact desorption (IID), in which adsorbates gain energy via electronic excitation or momentum transfer from plasma species, can occur.[37, 38] These processes promote desorption of surface species and free up active sites for reaction. Alternating removal and accumulation of surface poisoning hydrogen species would then respectively account for the slow evolution towards steady state conditions in the plasma on and plasma off conditions. A similar observation was made by Kumari *et al*. who noted a change in the open circuit voltage of their polymer electrolyte membrane reactor when exposed to a nitrogen plasma that relaxed back towards the initial value with the plasma turned off.[22] The interpretation presented here presumes that activated nitrogen reacts with protons on the Mo cathode surface. An alternative pathway, in which the plasma enhances the hydrogen evolution from the cathode and gaseous H_2 reacts with activated gas-phase nitrogen cannot be ruled out but is unlikely to be the dominant path to ammonia synthesis. This indirect pathway would require additional steps for H_2 bond formation and breaking and would be inconsistent with the observation of ready nitrogen incorporation into Mo under the action of the plasma (**Figure 2**).

View Article Online
DOI: 10.1039/D6SE00290K

The increase in current with the plasma on could alternatively be attributed to a simple heating effect. To evaluate this possibility, Schlieren imaging of the plasma jet was undertaken. The images (**Figure S4**) reveal that there is no detectable gradient in the refractive index of the plasma plume or surrounding gas with the plasma on or off. This result indicates that the temperature remains relatively constant and rules out the possibility that the increase in the current density with the plasma on is due to an increase in cell temperature.

The overall low Faradaic efficiency (1.9% ± 0.7%) in the PCE condition indicates that a large portion of the current is directed towards the HER rather than the NRR. Delivery of hydrogen via electrochemical pumping over solid acid electrochemical cells has been demonstrated to occur with 100% Faradaic efficiency, and thus a high rate of HER in the present system would not be surprising.[39] The NH_3 production rate of 1.2 ± 0.5 nmol $NH_3/s{\cdot}cm^2$ in the PCE condition corresponds to a partial current density of 0.35 mA/cm^2. This is far less than the ~ 5 mA/cm^2 mean increase in current density between the electrochemistry-only and PCE conditions (**Figure 4a**) and suggests that not only is the rate of the competing HER high, it is also enhanced in the presence of the N_2/Ar plasma. If true, alternating between plasma activation to generate reactive nitrogen species on the cathode surface and electrochemical bias to drive protons towards reaction sites emerges as a future strategy for enhancing the conversion of bias-driven current into NH_3. Beyond Faradaic efficiency, energy consumption is an important metric in assessing the eventual viability of this PCE ammonia synthesis process. In the present system, the energy input relative to ammonia produced is 6 ± 2 MWh/mol NH_3. The plasma accounts for 99.85% of the total energy consumed, indicating that efficiency gains may be possible from optimizing plasma operating parameters such as specific energy input and plasma pulse source, which were not extensively explored here.

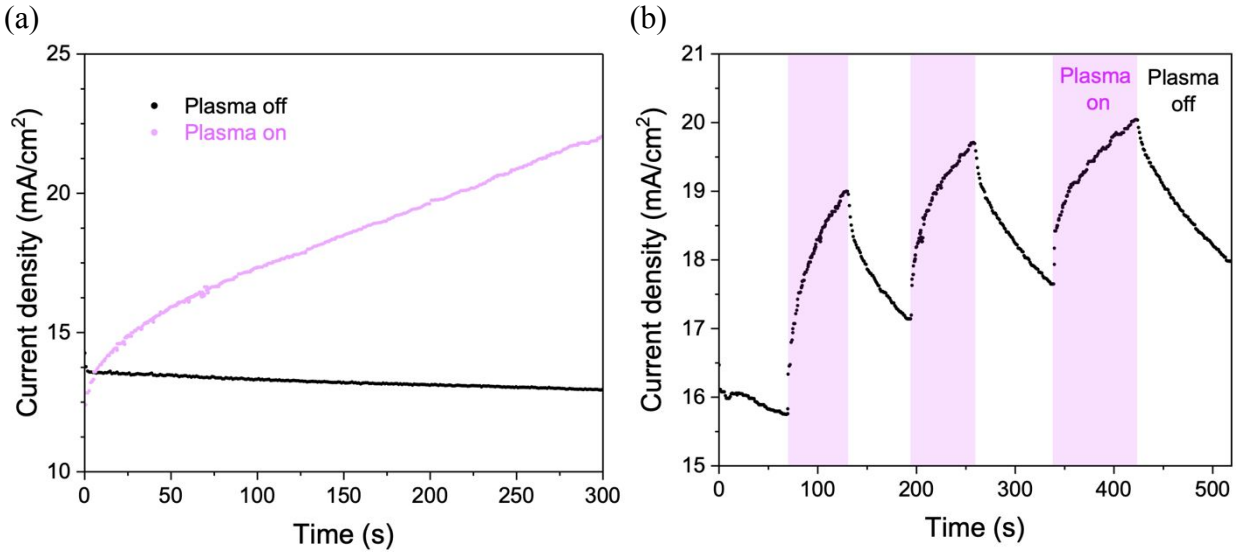

***Figure 4**. Electrochemical response in the form of chronoamperograms of ammonia electrochemical synthesis cells operated at -2 V, with and without plasma activation: (a) with a rest period of several minutes between the plasma off and on conditions; and (b) with continuous alternation between plasma off and on conditions.*

View Article Online
DOI: 10.1039/D6SE00290K

Conclusions

Direct plasma-coupled electrochemical ammonia synthesis using a solid acid electrochemical cell outfitted with a molybdenum cathode and a N_2/Ar plasma jet at 140 °C achieves an ammonia production rate of 1.2 ± 0.5 nmol $NH_3/s \cdot cm^2$ and Faradaic efficiency of 1.9% ± 0.7%. No ammonia synthesis is observed when only an electrochemical bias is used. XPS analysis of the Mo surface after exposure to a nitrogen plasma suggests the plasma activation of N_2 enhances its ability to bind to the surface of the Mo cathode, facilitating the reaction pathway from gaseous N_2 to NH_3. The high sensitivity of Mo oxidation in the presence of even low concentrations of oxygen during plasma activation motivates use of an oxygen-free environment at the cathode. This constraint is addressed by employing the solid acid electrolyte, $Cs_7(H_4PO_4)(H_2PO_4)_8$, which is stable in its superprotonic state under air-free, dry conditions. Comparison of the current with and without plasma activation to the ammonia synthesis rate indicates the plasma not only helps to facilitate the NRR, but catalyzes the HER as well. Although the reactor design and operation have not been optimized in this study, there are ample opportunities in future works to improve the synthesis rate, Faradaic efficiency, and energy efficiency through tuning of the extensive array of parameters that impact the performance of the PCE reactor. Even in the absence of these optimization steps, the successful engineering of this reactor provides a basic framework of an electrified technology with several practical advantages. The use of a plasma jet is particularly advantageous because it delivers a high, localized flux of reactive plasma species directly to the cathode surface, enhancing interfacial reaction rates while minimizing bulk losses. In addition, this approach offers significant practical benefits compared to state-of-the-art plasma-electrochemical ammonia synthesis systems that require vacuum operation[20] or complex two-step tandem liquid-phase reactor configurations.[16, 17] Our platform instead operates under ambient pressure and in the gas phase, providing a simpler, more scalable architecture with fewer engineering constraints and lower balance-of-plant demands. Overall, this work provides insight into the interplay between plasma activation and electrocatalysis and establishes a foundation for further investigation into intermediate temperature plasma-coupled electrochemistry.

Author contributions

Dylan Bardgett performed conceptualization, data curation, formal analysis, methodology and investigation, project administration, resource management, visualization, and writing/editing for the original draft. James Ho performed formal analysis, investigation, resource management, visualization, and writing, reviewing, and editing. Dayne Swearer and Sossina Haile both contributed to conceptualization, funding acquisition, supervision, and the reviewing and editing process.

Conflicts of Interest

There are no conflicts to declare.

View Article Online
DOI: 10.1039/D6SE00290K

Data availability

Data for this article, including X-ray (XPS, XRR, XRD), electrochemical (EIS, chronoamperograms), and raw UV-Vis data from the salicylate method are available on the Open Science Framework at https://osf.io/meb85/overview?view_only=618cfe40613f494c93903cc1e13ae187 (private link for reviewers, DOI available upon acceptance). Supplementary Information (SI) is available. See DOI: References 23, 30, 40, and 41 are cited in the Supplementary Information.

Acknowledgements

D.F.S. acknowledges support from the U.S. Army DEVCOM ARL Army Research Office (ARO) Energy Sciences Competency, Electrochemistry Program award # W911NF-25-1-0026. The views and conclusions contained in this document are those of the authors and should not be interpreted as representing the official policies, either expressed or implied, of the U.S. Army or the U.S. Government. This research was supported by the Trienens Institute for Sustainability and Energy at Northwestern University. This work made use of the NUFAB (RRID: SCR_017779), Keck-II (RRID: SCR_026360), EPIC (RRID: SCR_026361), and Jerome B. Cohen X-ray Diffraction Core (RRID: SCR_017866) facilities of Northwestern University's NUANCE Center and Materials Research Center, which have received support from the SHyNE Resource (NSF ECCS-2025633), the IIN, and Northwestern's MRSEC program (NSF DMR-2308691). D.B.'s contributions were additionally supported by the National Science Foundation Graduate Research Fellowship under Grant No. DGE-2234667. J.H acknowledges funding support from the Northwestern University Ryan Fellowship and technical support with Schlieren imaging from Alexander Davis.

References

(1) Lamb, K. E.; Dolan, M. D.; Kennedy, D. F. Ammonia for hydrogen storage; A review of catalytic ammonia decomposition and hydrogen separation and purification. *Int. J. Hydrog. Energy* **2019**, *44*, 3580-3593. DOI: 10.1016/j.ijhydene.2018.12.024.
(2) Lim, J.; Fernández, C. A.; Lee, S. W.; Hatzell, M. C. Ammonia and Nitric Acid Demands for Fertilizer Use in 2050. *ACS Energy Lett.* **2021**, *6*, 3676−3685. DOI: 10.1021/acsenergylett.1c01614.
(3) Hochman, G.; Goldman, A. S.; Felder, F. A.; Mayer, J. M.; Miller, A. J. M.; Holland, P. L.; Goldman, L. A.; Manocha, P.; Song, Z.; Aleti, S. Potential Economic Feasibility of Direct Electrochemical Nitrogen Reduction as a Route to Ammonia. *ACS Sustain. Chem. Eng.* **2020**, *8*, 8938-8948. DOI: 10.1021/acssuschemeng.0c01206.
(4) Qing, G.; Ghazfar, R.; Jackowski, S. T.; Habibzadeh, F.; Ashtiani, M. M.; Chen, C.-P.; Milton R. Smith, I.; Hamann, T. W. Recent Advances and Challenges of Electrocatalytic N2 Reduction to Ammonia. *Chem. Rev.* **2020**, *120*, 5437-5516. DOI: 10.1021/acs.chemrev.9b00659.
(5) Marnellos, G.; Stoukides, M. Ammonia Synthesis at Atmospheric Pressure. *Science* **1998**, *282*, 98-100. DOI: 10.1126/science.282.5386.98.
(6) Choi, J.; Suryanto, B. H. R.; Wang, D.; Du, H.-L.; Hodgetts, R. Y.; Vallana, F. M. F.; MacFarlane, D. R.; Simonov, A. N. Identification and elimination of false positives in

View Article Online
DOI: 10.1039/D6SE00290K

electrochemical nitrogen reduction studies. *Nat. Commun.* **2020**, *11*, 5546. DOI: 10.1038/s41467-020-19130-z.
(7) Du, H.-L.; Gengenbach, T. R.; Hodgetts, R.; MacFarlane, D. R.; Simonov, A. N. Critical Assessment of the Electrocatalytic Activity of Vanadium and Niobium Nitrides toward Dinitrogen Reduction to Ammonia. *ACS Sustain. Chem. Eng.* **2019**, *7*, 6839-6850. DOI: 10.1021/acssuschemeng.8b06163.
(8) Andersen, S. Z.; Čolić, V.; Yang, S.; Schwalbe, J. A.; Nielander, A. C.; Mcenaney, J. M.; Enemark-Rasmussen, K.; Baker, J. G.; Singh, A. r.; rohr, B. A.; et al. A rigorous electrochemical ammonia synthesis protocol with quantitative isotope measurements. *Nature* **2019**, *570*, 504-508. DOI: 10.1038/s41586-019-1260-x.
(9) Hu, B.; Hu, M.; Seefeldt, L.; Liu, T. L. Electrochemical Dinitrogen Reduction to Ammonia by Mo2N: Catalysis or Decomposition? *ACS Energy Lett.* **2019**, *4*, 1053-1054. DOI: 10.1021/acsenergylett.9b00648.
(10) Hanifpour, F.; Canales, C. P.; Fridriksson, E. G.; Sveinbjörnsson, A.; Tryggvason, T. K.; Yang, J.; Arthur, C.; Jónsdóttir, S. ð.; Garden, A. L.; Ólafsson, S.; et al. Operando quantification of ammonia produced from computationally-derived transition metal nitride electro-catalysts. *J. Catal.* **2022**, *413*, 956-967. DOI: 10.1016/j.jcat.2022.07.030.
(11) Yesudoss, D. K.; Lai, H.-E.; Johnson, D.; Lee, M.; Reinhart, B.; Balbuena, P. B.; Djire, A. Lattice-Nitrogen-Mediated Chemistry Suppresses Hydrogen Evolution for Record Faradaic Efficiency in Ammonia Synthesis. *J. Am. Chem. Soc.* **2025**, *147*, 29327−29339. DOI: 10.1021/jacs.5c09104.
(12) Lefferts, L. Leveraging Expertise in Thermal Catalysis to Understand Plasma Catalysis. *Angew. Chem.* **2024**, *136*, e202305322. DOI: doi.org/10.1002/anie.202305322.
(13) Mehta, P.; Barboun, P.; Herrera, F. A.; Kim, J.; Rumbach, P.; Go, D. B.; Hicks, J. C.; Schneider, W. F. Overcoming ammonia synthesis scaling relations with plasma-enabled catalysis. *Nat. Catal.* **2018**, *1*, 269-275. DOI: 10.1038/s41929-018-0045-1.
(14) Wang, Y.; Craven, M.; Yu, X.; Ding, J.; Bryant, P.; Huang, J.; Tu, X. Plasma-Enhanced Catalytic Synthesis of Ammonia over a Ni/Al2O3 Catalyst at Near-Room Temperature: Insights into the Importance of the Catalyst Surface on the Reaction Mechanism. *ACS Catal.* **2019**, *9*, 10780-10793. DOI: 10.1021/acscatal.9b02538.
(15) Winter, L. R.; Chen, J. G. N2 Fixation by Plasma-Activated Processes. *Joule* **2021**, *5*, 300-315. DOI: 10.1016/j.joule.2020.11.009.
(16) Sun, J.; Zhou, R.; Hong, J.; Gao, Y.; Qu, Z.; Liu, Z.; Liu, D.; Zhang, T.; Zhou, R.; Ostrikov, K. K.; et al. Sustainable ammonia production via nanosecond-pulsed plasma oxidation and electrocatalytic reduction. *Appl. Cat. B: Environ.* **2024**, *342*, 123426. DOI: 10.1016/j.apcatb.2023.123426.
(17) Sun, J.; Alam, D.; Daiyan, R.; Masood, H.; Zhang, T.; Zhou, R.; Cullen, P. J.; Lovell, E. C.; Jalili, A. R.; Amal, R. A hybrid plasma electrocatalytic process for sustainable ammonia production. *Energy Environ. Sci.* **2021**, *14* (2), 865-872. DOI: 10.1039/D0EE03769A.
(18) Mohammad, A. F.; Al-Marzouqi, A. H.; El-Naas, M. H.; Bruggen, B. V. d.; Al-Marzouqi, M. H. A New Process for the Recovery of Ammonia from Ammoniated High-Salinity Brine. *Sustainability* **2021**, *13*, 10014. DOI: 10.3390/su131810014.

View Article Online
DOI: 10.1039/D6SE00290K

(19) Kumari, S.; Pishgar, S.; Schwartig, M. E.; Paxton, W. F.; Spurgeon, J. M. Synergistic Plasma-Assisted Electrochemical Reduction of Nitrogen to Ammonia. *Chem. Commun.* **2018**, *54*, 13347-13350. DOI: 10.1039/c8cc07869f.
(20) Sharma, R. K.; Patel, H.; Mushtaq, U.; Kyriakou, V.; Zafeiropoulos, G.; Peeters, F.; Welzel, S.; Sanden, M. C. M. v. d.; Tsampas, M. N. Plasma Activated Electrochemical Ammonia Synthesis from Nitrogen and Water. *ACS Energy Lett.* **2021**, *6*, 313-319. DOI: 10.1021/acsenergylett.0c02349.
(21) Baranov, A. I. Crystals with Disordered Hydrogen-Bond Networks and Superprotonic Conductivity. Review. *Crystallogr. Rep.* **2003**, *48*, 1012-1037.
(22) Sudesh, K.; Sahar, P.; Schwartig, M. E.; Paxton, W. F.; Spurgeon, J. M. Synergistic Plasma-Assisted Electrochemical Reduction of Nitrogen to Ammonia. *Chem. Commun.* **2018**, *54*, 13347-13350. DOI: 10.1039/c8cc07869f.
(23) Louis S. Wang; Patel, S. V.; Sanghvi, S. S.; Hu, Y.-Y.; Haile, S. M. Structure and Properties of Cs7(H4PO4)(H2PO4)8: A New + Superprotonic Solid Acid Featuring the Unusual Polycation (H4PO4). *J. Am. Chem. Soc.* **2020**, *142*, 19992-20001. DOI: 10.1021/jacs.0c08870.
(24) Anitha, V. P.; Major, S.; Chandrashekharam, D.; Bhatnagar, M. Deposition of Molybdenum Nitride Thin Films by R.F. Reactive Magnetron Sputtering. *Surf. Coat. Tech.* **1996**, *79*, 50-54.
(25) Wang, Y.; Lin, R. Y. Amorphous molybdenum nitride thin films prepared by reactive sputter deposition. *Mat. Sci. Eng. B* **2004**, *112*, 42-49. DOI: 10.1016/j.mseb.2004.05.010.
(26) Bagger, A.; Tort, R.; Titirici, M.-M.; Walsh, A.; Stephens, I. E. L. Electrochemical Nitrogen Reduction: The Energetic Distance to Lithium. *ACS Energy Lett.* **2024**, *9*, 4947-4952. DOI: 10.1021/acsenergylett.4c01638.
(27) Skúlason, E.; Bligaard, T.; Gudmundsdóttir, S.; Studt, F.; Rossmeisl, J.; Abild-Pedersen, F.; Vegge, T.; Jónsson, H.; Nørskov, J. K. A theoretical evaluation of possible transition metal electro-catalysts for N2 reduction. *Phys. Chem. Chem. Phys.* **2012**, *14*, 1235-1245. DOI: 10.1039/c1cp22271f.
(28) Richards, C.; Jans, E.; Gulko, I.; Orr, K.; Adamovich, I. V. N vibrational excitation in atmospheric pressure ns pulse and RF plasma jets. *Plasma Sources Sci. Technol.* **2022**, *31*, 034001. DOI: 10.1088/1361-6595/ac4de0.
(29) Khan, F. U.; Rehman, N. U.; Naseer, S.; Naz, M. Y.; Khattak, N. A. D.; Zakaullah, M. Effect of Excitation and Vibrational Temperature on the Dissociation of Nitrogen Molecules in Ar-N2 Mixture RF Discharge. *Spectrosc. Lett.* **2011**, *44*, 194-202. DOI: 10.1080/00387010.2010.497527.
(30) Le, P. T. T.; Boyd, C. E. Comparison of Phenate and Salicylate Methods for Determination of Total Ammonia Nitrogen in Freshwater and Saline Water. *J. World Aquacult. Soc.* **2012**, *43* (6), 885-889.
(31) Davies, H. L.; Guerra, V.; Woude, M. v. d.; Gans, T.; O'Connell, D.; Gibson, A. R. Vibrational kinetics in repetitively pulsed atmospheric pressure nitrogen discharges: average-power-dependent switching behaviour. *Plasma Sources Sci. Technol.* **2023**, *32*, 014003. DOI: 10.1088/1361-6595/aca9f4.
(32) Es-Sebbar, E.-T.; Sarra-Bournet, C.; Naudé, N.; Massines, F. o.; Gherardi, N. Absolute nitrogen atom density measurements by two- photon laser-induced

View Article Online
DOI: 10.1039/D6SE00290K

fluorescence spectroscopy in atmospheric pressure dielectric barrier discharges of pure nitrogen. *J. Appl. Phys.* **2009**, *106*, 073302. DOI: 10.1063/1.3225569.
(33) Qayyum, A.; Zeb, S.; Naveed, M. A.; Rehman, N. U.; Ghauri, S. A.; Zakaullah, M. Optical emission spectroscopy of Ar–N2 mixture plasma. *J. Quant. Spectrosc. Radiat. Transf.* **2007**, *107* (3), 361-371.
(34) Pandey, S.; Goldfine, E. A.; Sinha, S.; Zhang, C.; Wenderott, J. K.; Kaczmarczyk, L.; Dabrowiecki, K.; Dravid, V. P.; González, G. B.; Haile, S. M. Steam-Assisted Ammonolysis of MoO2 as a Synthetic Pathway to Oxygenated δ-MoN. *Materials* **2025**, *18*, 2340. DOI: 10.3390/ ma18102340.
(35) Boysen, D. A.; Uda, T.; Chisholm, C. R. I.; Haile, S. M. High performance Solid Acid Fuel Cells through humidity stabilization. *Science* **2004**, *303*, 68-70. DOI: 10.1126/science.1090920.
(36) Tanabe, T.; Yamanishi, Y.; Imoto, S. Hydrogen permeation and diffusion in molybdenum. *J. Nucl. Mater.* **1992**, *191-194*, 439-443. DOI: 10.1016/S0022-3115(09)80083-4.
(37) Neyts, E. C. Plasma-Surface Interactions in Plasma Catalysis. *Plasma Chem. Plasma Process* **2016**, *36*, 185-212. DOI: 10.1007/s11090-015-9662-5.
(38) Menzel, D. Desorption Phenomena. In *Interactions on Metal Surfaces*, Gomer, R. Ed.; Topics in Applied Physics, Springer, 1975; pp 101-142.
(39) Lim, D.-K.; Plymill, A. B.; Paik, H.; Qian, X.; Zecevic, S.; Chisholm, C. R. I.; Haile, S. M. Solid Acid Electrochemical Cell for the Production of Hydrogen from Ammonia. *Joule* **2020**, *4*, 2338-2347. DOI: 10.1016/j.joule.2020.10.006.
(40) Nelson, A. Co-refinement of multiple-contrast neutron/X-ray reflectivity data using MOTOFIT. *J. Appl. Crystallogr.* **2006**, *39*, 273-276. DOI: 10.1107/S0021889806005073.
(41) Le, P. T. T.; Boyd, C. E. Comparison of Phenate and Salicylate Methods for Determination of Total Ammonia Nitrogen in Freshwater and Saline Water. *J. World Aquacult. Soc.* **2012**, *43* (6), 885-889.

View Article Online
DOI: 10.1039/D6SE00290K

Plasma-coupled Electrochemical Ammonia Synthesis Using a Solid Acid Electrochemical Cell

Dylan Bardgett, James Ho, Dayne F. Swearer, Sossina Haile

Data availability

Data for this article, including X-ray (XPS, XRR, XRD), electrochemical (EIS, chronoamperograms), and raw UV-Vis data from the salicylate method are available on the Open Science Framework at https://osf.io/meb85/overview?view_only=618cfe40613f494c93903cc1e13ae187 (private link for reviewers, DOI available upon acceptance). Supplementary Information (SI) is available. See DOI: References 23, 30, 40, and 41 are cited in the Supplementary Information.